Enhancement of Placement Accuracy for SMD via Development of a New Illumination System

Kuk Won Ko[a], Jae Wan Kim[a], Hyung S. Cho[a],
Ki Soo Jin[b], Kwang Il Ko[b]

[a]Department of Mechanical Engineering, Korea Advanced Institute of Science and Technology
[b]Research and Development Center, Mirae Cooperation, LTD

ABSTRACT

Ever since surface-mounting technology (SMT) for printed circuit board (PCB) assembly processes has been developed, electrical products continuously tend toward the miniaturization of components, with denser packing of its boards. With the increasing necessity for reliable PCB product, there has been a considerable demand for high speed, high precision vision system to place the electric parts on PCB automatically. To recognize the electric parts with high accuracy and reliability, illumination condition is instrumental to acquisition of part images. In this paper, a versatile lighting is developed which utilizes three different types of illuminating methods: direct, indirect, and back-light illumination. The direct illumination uses to recognize the flat and specular surface of electric parts such as lead, and indirect illumination to recognize the lambertian surface or curved specular surface such as J-lead, BGA ball and gull-wing type lead. Finally, the back-light illumination is used to extract the orientation and location of the electric parts from acquired image. The recognition algorithm, since geometry and dimension vary with part, has been also developed for various electric parts. The recognition algorithm consists of two different image processing methods. One is binary image based algorithm to increase the speed of image processing algorithm and to recognize parts and defects, and the other is gray-level based algorithm to increase the accuracy of recognized parts pose. The performances of the developed vision system and recognition algorithm are tested on a number of samples of the electric parts used for PCB board. Experimental results reveal that the proposed system recognizes various type of electric parts with good accuracy and fast speed.

Keywords : Surface mount device, placement machine, visual recognition, backlight, integrated illumination system.

1. INTRODUCTION

Surface mount technology(SMT) has been originally developed in the mid 1960's in part to overcome some of the limitations of through hole assembly technology and more recently, surface mounting has become a popular technique for connecting a electronic. Components are soldered directly onto metal pads on the surface of the board without the use of through holes. Surface-mount devices are typically smaller than the through hole-typed counterparts and allow their board density higher. The popular surface mount electronic components are the plastic-leaded chip carrier(PLCC), the small-outline integrated circuit(SOIC), chip capacitor, chip resistor, ball grid array, and chip scale package(CSP).

The major processes in SMT assembly process include application of solder paste, component placement, reflow or wave soldering and surface cleaning. In the component placement process which is our topic in this paper, as shown in figure 1, the electric components is picked up from a feeder via a vacuum spindle and head(referred as a nozzle), and are aligned to proper orientation and location and are then placed properly on the PCB upon release of the vacuum. The alignment process is very important to guarantee the placement accuracy. Two types of alignment are accomplished either by mechanical means or with the aid of machine vision. In these days, SMD components show smaller pins and narrow space between pins so that even a very precise mechanical placement is considered to be not accuracy enough. Furthermore, the printed circuit board can be slightly dilated by small change of condition of environment such as temperature. For this reason, relative position of pins and footprints on PCB is relevant and therefore, vision system is required to feedback the relative

positioning error. The vision system is widely used not only to measure the pose of components relative to the center of picker, but also to inspect the defects of the picked component such as cracks, pitting, or chipping, missing lead, and the verification of component presence in the assembly.

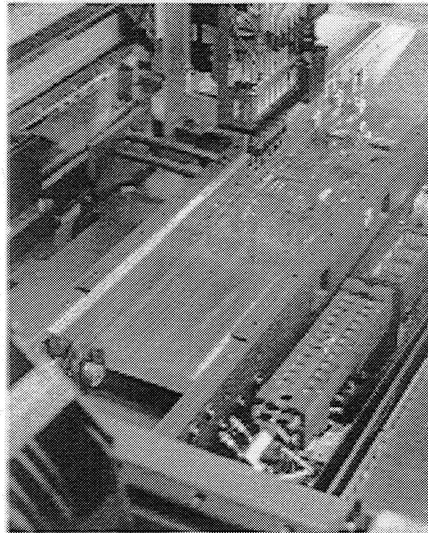

Figure 1. Surface mount placement process

In the vision system, acquiring a good quality image is very important in the placement of surface mount devices, since subsequent image processing depends on the quality of acquired image to reduce the noise. Here, illumination technique plays an important role in the acquisition of a high-quality image. However, types of SMD components exceed more 30, and the features of each component vary. In components such as QFP and SOIC with gull-wing type of lead, lead position is an important feature and direct illumination technique is one of a good solution. On the contrary, with direct illumination, the components with J-type of lead, stable features are difficult to acquire from captured image because highlight patterns in the image are only near flat part of J-type lead.

To accommodate the various types of SMD component, a versatile vision system is developed, that is equipped with three different types of illuminating devices: direct, indirect, and back-light illumination The direct illumination is used to recognize flat and specular surface of electric parts such as lead, and indirect illumination to recognize lambertian surface or curved specular surface such as J-lead, BGA or CSP ball and gull-wing type lead. Finally, back-light illumination is used to extract the orientation and location of electric parts from acquired image. Utilizing these illumination systems various vision algorithms are developed to measure the relative position and orientation of components and to inspect their defects.

The performances of the developed vision system and vision algorithm are tested on a number of samples of the SMD components. Experimental results show that the proposed system can works well for various types of electric parts with good accuracy and speed.

2. ILLUMINATION SYSTEM

In figure 2, a schematic is shown for the developed illumination system. It consists of three different types of illumination devices employing direct illumination, indirect illumination, back-light illumination, a CCD camera with zoom lens giving a minimum field of view of approximately from 4mm x 4mm to 40 mm x40mm. The LED is selected as an illumination source because the light intensity is easily controlled.

The schematics of three types of illumination are shown in figure 3. The direct illumination system is based on co-axial illumination and is constructed by using a half-mirror. The target of direct illumination is the flat and specular surface of SMD components such as lead and body. The only flat surface reflects the ray from direct illumination into camera directly and high light patterns are acquired. The efficient area of the illumination is 40mm x 40mm in size and the focal area which has same light intensity is 30mm x 30mm. Figure 3 shows three different types of illumination methods.

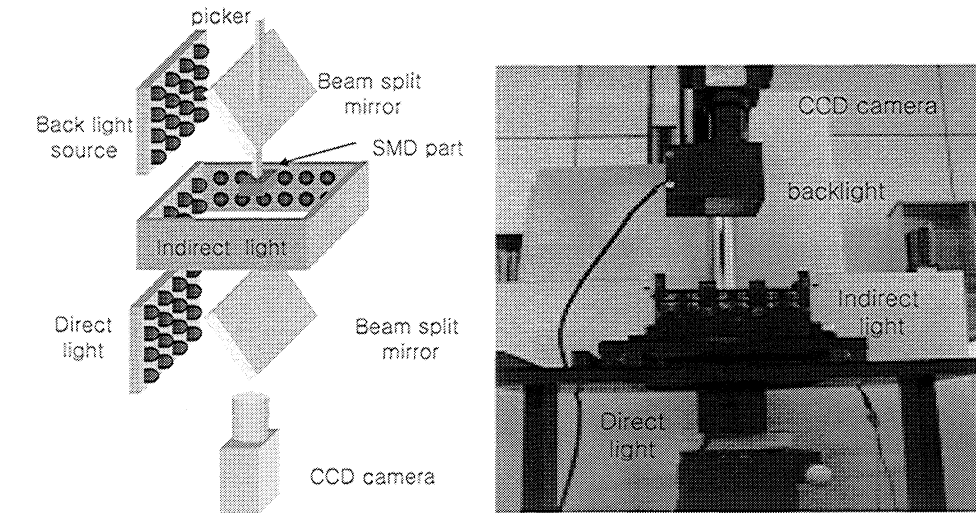

Figure 2 The schematic of the proposed illumination system

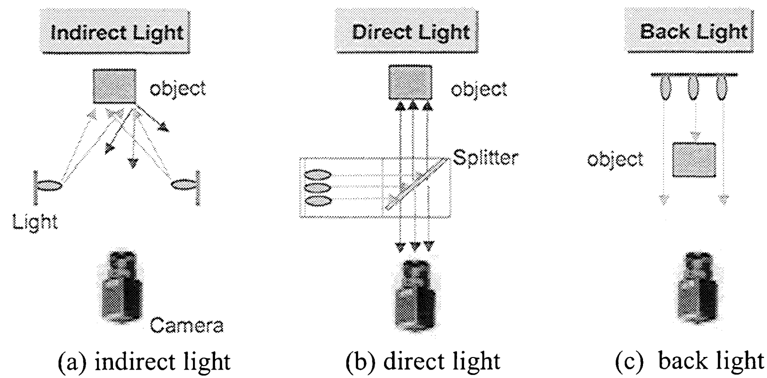

Figure 3. Three types of illumination methods

The curved surface such as J-type lead, BGA ball and so on, is captured by indirect illumination. The ray from indirect illumination reflects curved surface and goes into CCD camera. The indirect illumination generated by an array of SMD chip leads which has 3000 mili-candela light intensity. The incident angle of indirect system is important because reflected ray from curved surface goes into CCD camera. The incident angle in indirect illumination is selected from 15° to 35° from the consideration of the surface angle distribution on the previous study[10,11]. The intensity distribution of indirect system is tested by capturing images on the lambertian surface and is shown in figure 4. The result shows the light distribution is approximately uniform throughtout the field of camera view.

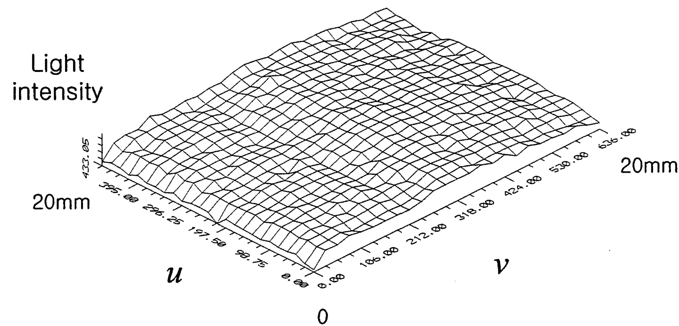

Figure 4. The light intensity distribution

The backlight system can not easily implemented because light source are attached to the picker. The weight of picker is an important fact influencing the speed of picker movement. To reduce the weight of picker, the back light source is attached vertically to the direct and indirect illumination system, and the only half mirror is attached to the picker as shown in Fig 2. The light is reflected to half mirror and goes into the camera directly. By using the beam split mirror, the light source are separated from the jig.

3. VISION ALGORITHM

In this chapter, we introduce the vision algorithms to determine the position and orientation of three different types of components which are frequently being used for PCB packaging ; SOIJ(QFP), TR, BGA. The image processing algorithm consists of two different image processing methods. One is the binary image based algorithm to increase the speed of image processing algorithm and to recognize parts and defects, and the other is the gray-level based algorithm to increase the accuracy of parts pose. The vision algorithms developed for each electronic component are explained in the subsequent sections.

3.1. Vision algorithm for SOIJ

J-lead type SOIJ is shown in figure 5, the J-type leads are attached to both sides of the package with a certain lead width and pitch. In the case of SOIJ, the number of leads, the lead pitch, the lead width, chip position and orientation are the major information extracted by the vision algorithm.

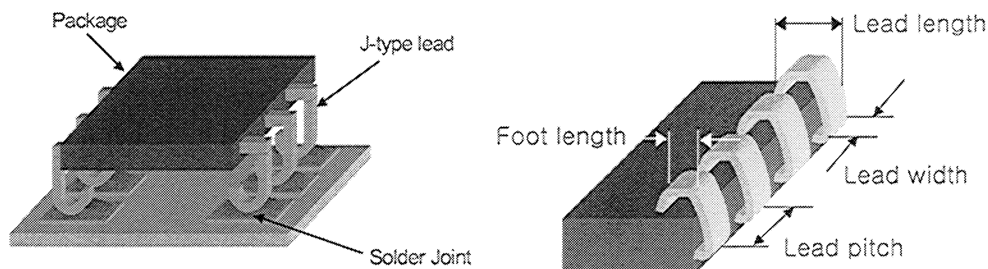

Figure 5. SOIJ and the extracted information

1) Orientation and location of the component

The back lighting method is used to determine the chip orientation and location. Figure 6(a) shows the back lighting image of SOIJ. As can be seen, the image by back lighting method is highly contrasted. The major feature in this image type is the edge of the package. The edge detection method with Sobel operator is applied to the back lighting image, and the processed image is shown in figure 6(b). To obtain the chip orientation and location, edge line of the component body is obtained. The vision algorithm composed of two parts: a moment-based method and Hough transform-based method is applied. Using the extracted edge information, a moment-based method is firstly applied to the edge image. Orientation is defined as the angle of axis of the least moment of inertia. It is obtained by minimizing the moment of inertia with respect to the angle. Location is defined as the center of mass. The detailed description for the moment-based method has been presented in reference [13]. Secondly, Hough-transform method is applied to find the line feature of the chip body in the edge image. Through the obtained line information, the chip orientation and location are calculated again. By using the moment and the line informations, we can find more accurate posture parameters.

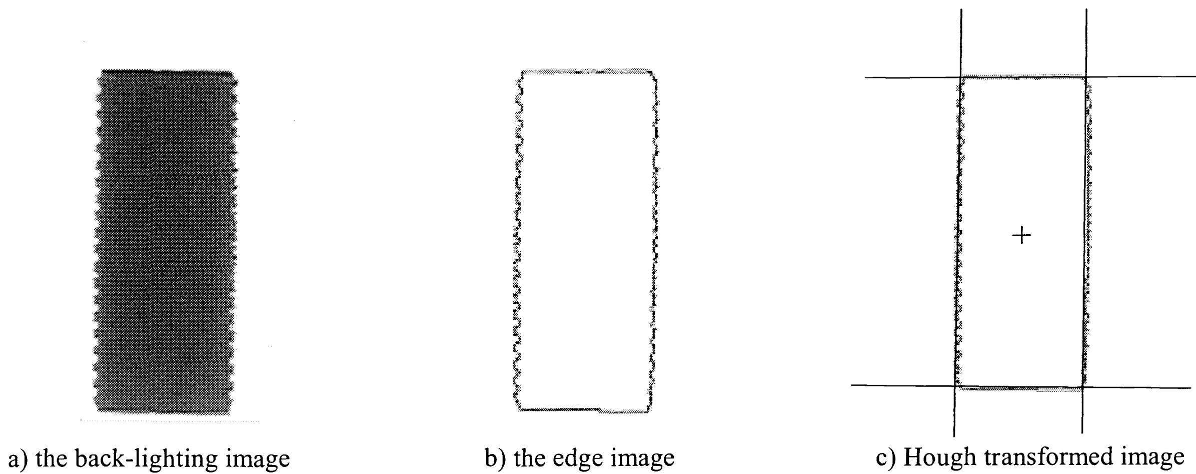

a) the back-lighting image b) the edge image c) Hough transformed image

Figure 6. the back-lighting image & the edge image

2) Lead inspection

Because J-type lead has the curved shape, both direct and indirect illuminations are applied for inspecting the leads. Figures 7 and 8 show the captured image and the flow chart of the SOIJ inspection algorithm, respectively. In the image, the highlight patterns are the chip leads. It is observed that the background and the chip body are not distinctly divided. The captured image is firstly binarized by optimal thresholding technique [13], and then the white objects in the binarized image are blobbed and labeled. Secondly, the centroid of each white blob is calculated to find the position of each lead.

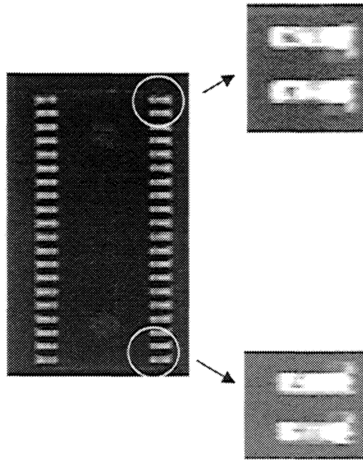

Figure 7. The captured image to inspection J-type lead

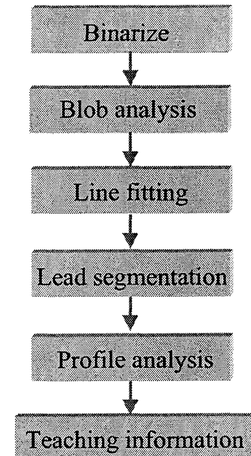

Figure 8. SOIJ inspection algorithm

In figure 9, the pre-processed images are shown. The obtained centroids are used to classify the blobs into two groups: left/right lead array. All lead centroids are fitted to a line based on least square error method. The line fitting method is as follow:

$$
\begin{aligned}
u &= av + b \\
a &= (N \times \bar{U}\bar{V} - \overline{UV}) / (N \times \overline{V^2} - \bar{V}^2) \\
b &= (\bar{U}\overline{V^2} - \overline{UV} \times \bar{V}) / (N \times \overline{V^2} - \bar{V}^2)
\end{aligned}
\tag{1}
$$

where $\overline{UV} = \sum_{i=1}^{N} u_i v_i$, $\bar{U} = \sum_{i=1}^{N} u_i$, $\bar{V} = \sum_{i=1}^{N} v_i$, $\overline{V^2} = \sum_{i=1}^{N} v_i^2$, u and v is the coordinate values of the blob center, and N denotes total number of leads. Left/right array can be recognized through determining whether each lead is on left or right of this line.

From the classified results, each lead array is fitted to a line for the profile analysis. It is shown in figure 9(a). Figure 9 (b) show the intensity variation along these lines. By analyzing the intensity profile, we can obtain the information of the lead width, lead pitch, and foot length. The thresholding value is acquired by the above mentioned optimal thresholding technique. From the prior knowledge of the total lead number, the lead width and pitch are easily calculated.

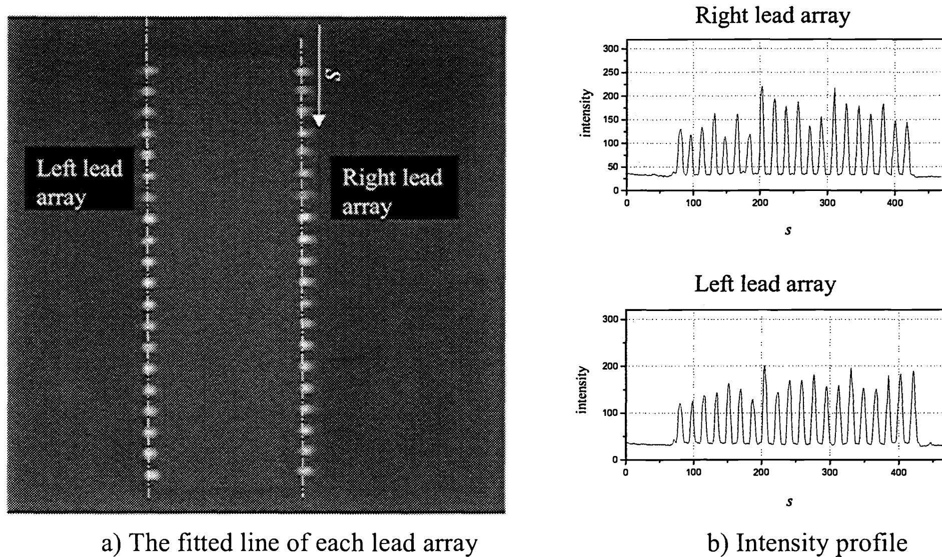

Figure 9. Intensity variation along the fitted line of each lead array

3.2 Vision algorithm for TR

TR component is shown in figure 10. The flat leads are attached to both sides of the package. The number of lead, locations of each lead, the orientation and positions of components are the major parameters to be extracted by the proposed vision algorithm.

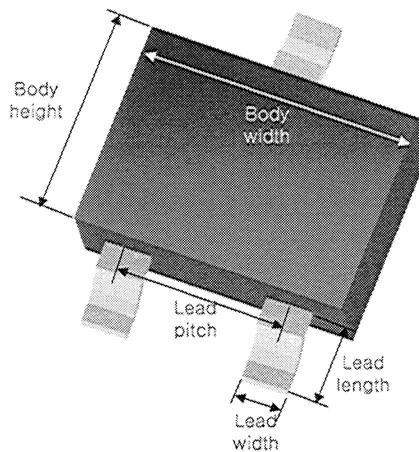

Figure 10. TR and the parameters to be determined

1) The component orientation and locations

The backlighting image of TR is shown in figure 11(a). After the image is captured, the edge is extracted by a simple sobel operation. Figure 14(b) shows the edge images. Hough transform is applied to the edge image, which is frequently used to

detect line. Its advantage is that it is relatively unaffected by gaps in line and by noise. The figure (c) show the result of line matching by hough transform. The center location (x_{tr}, y_{tr}) and orientation (θ_{tr}) are calculated from the four lines expressed by (*a,b : y=ax+b*). To find the center coordinates of the TR body, the intersection points of two adjacent lines are calculated. The intersection points (x_i^*, y_i^*) of two adjacent line is expressed by equation (2). The center coordinates of TR are calculated by the average of the four intersection points. The rotation angle θ_{tr} is calculated from the average gradient of two long line shown in figure 11(c).

$$\begin{bmatrix} x_i^* \\ y_i^* \end{bmatrix} = \begin{bmatrix} a_1 & -1 \\ a_2 & -1 \end{bmatrix}^{-1} \cdot \begin{bmatrix} b_1 \\ b_2 \end{bmatrix} \qquad (2)$$

where x_i^* and y_i^* are the *i*th intersection point and a_1, a_2, b_1, b_2 are the line components of two adjacent lines.

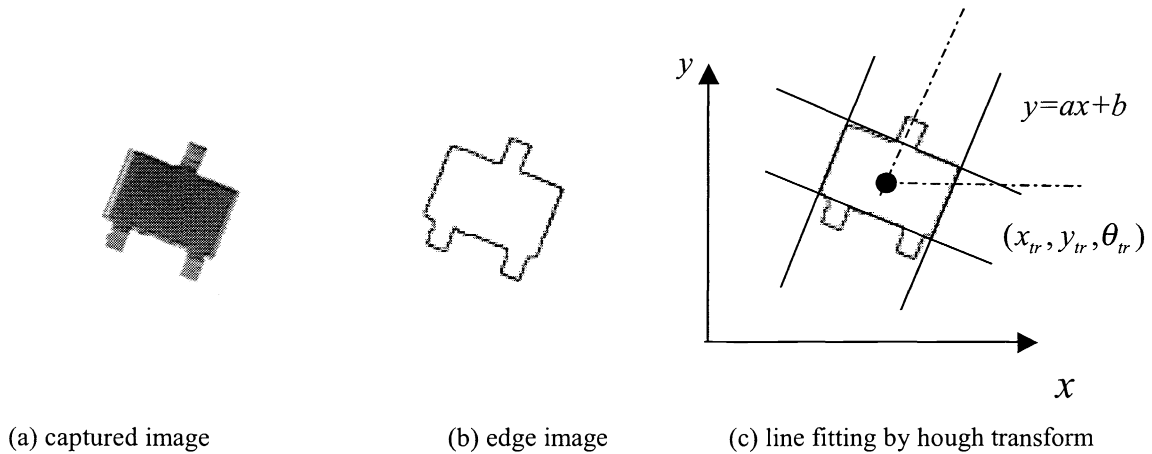

(a) captured image (b) edge image (c) line fitting by hough transform

Figure 11. Backlight image of a TR part

2) The lead length and width

When the image is input to the algorithm, then by performing thresholding, binary image is obtained and discriminantes leads from the background. Figure 12(a) shows the graylevel histogram. The graylevel distribution of lead is separated from that of body and background. In this process, adaptive optimal thresholding technique is applied since both images of lead and background are changing with illumination condition. The thresholding technique is based on nonparametric method[13]. The graylevel distribution is normalized and then, threshold value is calculated to maximize the variances of two graylevel disribution. The resultant binary image is shown in figure 12(b). After thresholding, the center of each blob is calculated through labeling method. To find the width and length of lead, the line fitting by hough transform is applied by using edge information of the TR lead and then, a similar image processing is done.

4. EXPERIMENTS AND DISCUSSIONS

4.1 Experimental conditions

To evaluate the performance of the proposed method, a series of experiments was performed for various types of SMD components. The proposed vision algorithm was tested for various orientations and locations and various contrast in image by changing light intensity. The calculated orientations and locations are compared to the predetermined orientation and position using the optical X-Y-θ optical jig.

The image calibration is performed by using well known camera model[12,13]. The camera calibration is to find the

relation ship between image coorniates (u,v) and world coordinates (x,y). The relation is expressed by

$$x = a_1u^3 + b_1u^2v + c_1uv^2 + d_1v^3 + e_1u^2 + f_1v^2 + g_1uv + h_1u + i_1v + j_1$$
$$y = a_2u^3 + b_2u^2v + c_2uv^2 + d_2v^3 + e_2u^2 + f_2v^2 + g_2uv + h_2u + i_2v + j_2 \quad (3)$$

and the above equation is also expressed by a matrix form, equation(4), and the 12 unknown parameters are found by using inverse transformation procedure. The chart used for the calibration and the calibration errors are shown in figure 13. The maximum calibration error is 0.0107 mm and the averaged error is 0.00526 within 10mm × 10mm FOV.

$$\begin{bmatrix} x_1 & y_1 \\ \vdots & \vdots \\ x_n & y_n \\ \vdots & \vdots \\ x_N & y_N \end{bmatrix} = \begin{bmatrix} u_1^3 & u_1^2v_1 & u_1v_1^2 & v_1^3 & u_1^2 & v_1^2 & u_1v_1 & u_1 & v_1 & 1 \\ \vdots & \vdots & \vdots & \vdots & \vdots & \vdots & \vdots & \vdots & \vdots & \vdots \\ u_n^3 & u_n^2v_n & u_nv_n^2 & v_n^3 & u_n^2 & v_n^2 & u_nv_n & u_n & v_n & 1 \\ \vdots & \vdots & \vdots & \vdots & \vdots & \vdots & \vdots & \vdots & \vdots & \vdots \\ u_N^3 & u_N^2v_N & u_Nv_N^2 & v_N^3 & u_N^2 & v_N^2 & u_Nv_N & u_N & v_N & 1 \end{bmatrix} \begin{bmatrix} a_1 & a_2 \\ b_1 & b_2 \\ c_1 & c_2 \\ d_1 & d_2 \\ e_1 & e_2 \\ f_1 & f_2 \\ g_1 & g_2 \\ h_1 & h_2 \\ i_1 & i_2 \\ j_1 & j_2 \end{bmatrix} \quad (4)$$

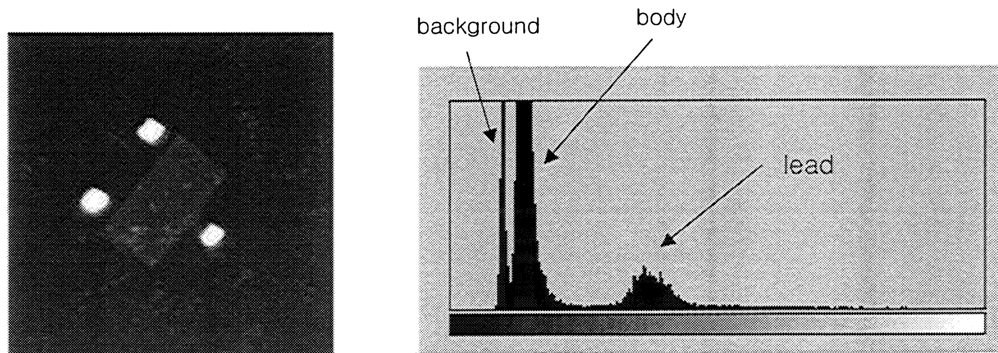

(a) Captured image and graylevel histogram of a TR part

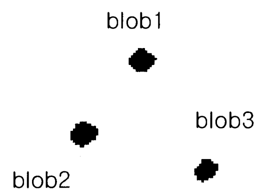

(b) binary image

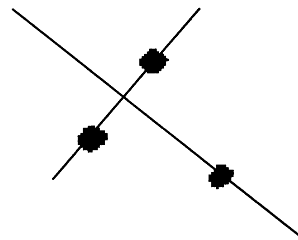
(c) center of each blob

Figure 12. The image processing of a TR part(continue)

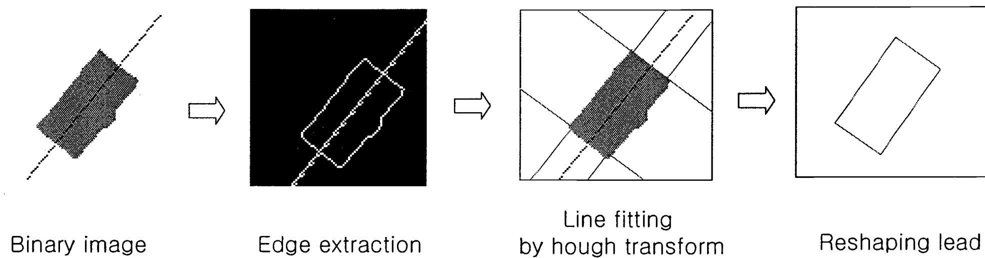

(d) image process for lead width and length

Figure 12. The image processing of a TR part

4.2 The results of orientation and rotation calculation

Table 1 shows the calculated errors obtained after reliability test of the proposed illumination system and vision algorithm. The 10 images for each component are captured in the same position. The processed images are used to extract lines and all orientations and locations are calculated. These experimental results show that the reliability of the proposed system is so good to guarantee 10% and 6.25% maximum errors for TR and SOIJ components, respectively.

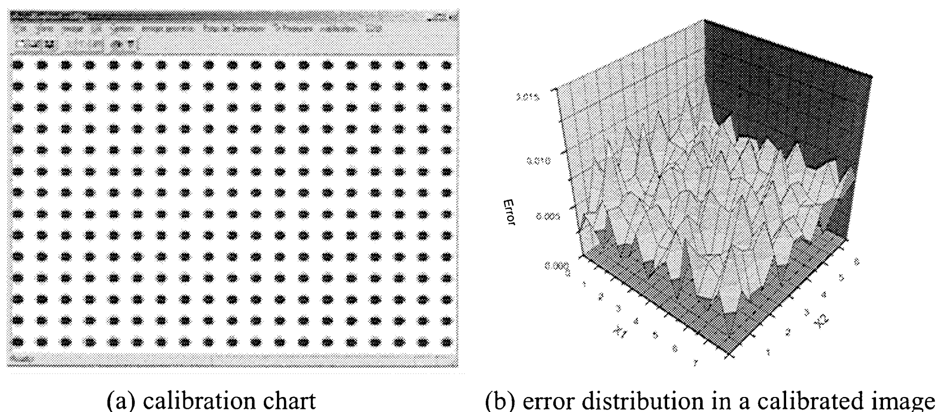

(a) calibration chart (b) error distribution in a calibrated image

Figure 13. The chart for calibration and the calibration results

Table 1. Reliability test for SOIJ and TR components

Trial 1	width of lead	length of lead	pitch of lead
1	0.52	1.08	1.27
2	0.53	1.08	1.27
3	0.52	1.08	1.27
4	0.52	1.08	1.27
5	0.52	1.08	1.27
6	0.51	1.08	1.27
7	0.52	1.08	1.27
8	0.52	1.08	1.27
9	0.52	1.08	1.27
10	0.51	1.08	1.27
CAD data	0.50	1.20	1.26
average	0.52	1.08	1.27
avg. error(mm)	0.01	−0.12	0.01
avg. error(%)	2.00	−10.00	0.79
max. error(mm)	0.01	0.12	0.02
max. error(%)	2.00	10.00	1.59

(a) experimental results of SOIJ

Trial 1	width of lead 1	width of lead 2	width of lead 3	Body width	Body height
1	0.36	0.33	0.32	1.75	1.17
2	0.34	0.35	0.32	1.74	1.18
3	0.35	0.32	0.32	1.76	1.18
4	0.36	0.34	0.33	1.77	1.18
5	0.36	0.34	0.32	1.75	1.19
6	0.35	0.33	0.32	1.73	1.17
7	0.36	0.32	0.33	1.75	1.20
8	0.36	0.34	0.33	1.76	1.17
9	0.36	0.33	0.34	1.77	1.18
10	0.35	0.33	0.32	1.75	1.17
CAD data	0.35	0.33	0.32	1.75	1.20
average	0.36	0.33	0.33	1.75	1.18
avg. error(mm)	0.01	0.00	0.01	0.00	0.02
avg. error(%)	2.86	0.00	3.13	0.00	1.67
max. error(mm)	0.01	0.02	0.02	0.02	0.03
max. error(%)	2.86	6.06	6.25	1.14	2.50

(b) experimental results of TR

The major features of SMD placement for accurate placement are the orientation and location. Table 2 shows the results of the orientations and locations of four components In these results appearing at table 2, the errors in each corner appear slightly larger than that of center because the corner images are slightly distorted even though camera calibration. The average errors of location and orientation are below 0.15mm and 0.08mm respectively. The experimental results show that the proposed vision system is accurate to place the components with 0.5mm fine pitch.

Table 2. Experimental results of location and orientation for SOIJ and TR components

Trial 3	x location	y location	angle
1	2.12	1.11	10.11
2	2.11	1.11	10.14
3	2.13	1.12	9.96
4	2.12	1.10	10.04
5	2.13	1.11	9.96
6	2.12	1.11	10.04
7	2.11	1.12	9.91
8	2.12	1.13	10.05
9	2.11	1.12	9.97
10	2.12	1.12	9.95
real position	2.12	1.12	10.00
average	2.12	1.11	10.02
avg. error(mm)	0.01	0.01	0.02
max. error(mm)	0.01	0.02	0.14

(a) position errors of SOIJ at center

Trial 3	x location	y location	angle
1	1.02	0.51	5.11
2	0.98	0.52	5.13
3	1.00	0.48	5.07
4	1.01	0.49	4.91
5	1.02	0.50	5.04
6	0.98	0.52	5.03
7	1.02	0.47	4.98
8	1.01	0.48	4.94
9	0.99	0.51	5.02
10	1.00	0.50	4.98
real position	1.00	0.50	5.00
average	1.00	0.50	5.03
avg. error(mm)	0.00	0.00	0.04
max. error(mm)	0.02	0.03	0.13

(b) position errors of TR at center

Trial 4	x location	y location	angle
1	1.53	1.51	15.11
2	1.57	1.54	15.19
3	1.49	1.52	14.89
4	1.43	1.53	15.06
5	1.51	1.49	14.91
6	1.44	1.44	14.98
7	1.48	1.54	15.13
8	1.49	1.51	14.90
9	1.49	1.55	14.97
10	1.51	1.43	15.12
real position	1.50	1.50	15.00
average	1.49	1.51	15.02
avg. error(mm)	0.01	0.01	0.02
max. error(mm)	0.07	0.07	0.19

(c) position errors of SOIJ at corner

Trial 4	x location	y location	angle
1	1.09	0.54	10.19
2	0.97	0.48	10.20
3	1.04	0.55	9.91
4	1.12	0.52	10.09
5	0.97	0.49	0.92
6	0.98	0.59	10.04
7	1.01	0.44	9.91
8	1.04	0.46	10.11
9	1.07	0.52	9.89
10	0.94	0.53	9.95
real position	1.00	0.50	10.00
average	1.02	0.51	9.03
avg. error(mm)	0.01	0.01	0.97
max. error(mm)	0.12	0.09	0.20

(d) position errors of TR at corner

5. CONCLUSIONS

In this paper, an automated vision system and vision algorithms for SMD placement machines has been developed. The integrated illumination system is developed. The developed vision system has three types of illumination methods and can acquire reliable features of various types of SMD components. This illuminant system was found to reduce image noise and enhance contrast.

The vision algorithm consists of two different image processing methods. One is the binary image based algorithm to increase the speed of image processing algorithm and to recognize parts and defects, while the other is the gray-level based algorithm to increase the accuracy of recognized parts pose.

To evaluate the performance of the proposed vision algorithms, a series of experiments was conducted for several types of components. The experimental results show the developed algorithm can measure the relative position and orientation with a good accuracy and fast processing time less than 100 millisececonds. They also show the robustness of the proposed algorithm in the presence of noisy and low constant images.

ACKNOWLEDGEMENTS

This work was supported by Mirae Corporation and conducted through 1999~2000. The authors would like to thank Dr. H .R. Beom of Mirae Corporation Company for his valuable advice.

REFERENCES

1. G. Burel, F. Bernard and W.J. Venema, "Vision feedback for SMD placement using neural network", *IEEE international conferenec of electronic packing*, pp 1491-1496,-1995.
2. Hwang, Jennie, S. "Modern solder technology for competitive electronics manufacturing", New York, *McGraw-Hill*, 1996.
3. Oakes Ian, " Management of Electronics Assembly", *Newton*, 1992.
4. Zussman, E., SMD placement on three-dimensional circuit board", *IEEE Transactions on Electronics Packaging Manufacturing*, Vol. 22 2 , pp. 147 –150, April 1999.
5. Capson, D.W.; Tsang, R.M.C, "An experimental vision system for SMD component placement inspection ", *IECON '90, 16th Annual Conference of IEEE*, Vol.1, pp. 815 –820, 1990.
6. Bartlett S.L, Besl. P.J, Jain R, Mukherjee. D and Skifstad K.D, "Automatic Solder Joint Inspection", *IEEE Trans, PAMI* , Vol. 10, No. 1 pp. 31-43, 1988.
7. Ikeuchhi, K., "Determining Surface Orientations of specular Surfaces by using the Photometric Stereo Method", *IEEE Trans PAMI*, Vol. 3, No. 6, pp 661-669, 1981.
8. Nayar S. K., Sandreson. A.C., Weiss L. E. and Simson D.D, "Specular Surface Inspection using Structured highlight and Gaussian Images", *IEEE Trans, Robotics and Automation*, Vol. 6, No. 2, pp. 108-218, 1990.
9. K.W. Ko and H.S. Cho, "Solder joints inspection using a neural network and fuzzy rule-based classification method", IEEE Trans. on Electronics Packing Manufacturing, Vol. 23, No. 2, pp. 93-103, 2000.
10. J.H. Kim and H.S. Cho, "Neural network based inspection of solder joints using a circular illumination", *Image and Vision Computing*, Vol. 13, No. 6, pp. 479-490, 1995.
11. Juyang Weng, Paul Cohen and Marc Herniou, " Camera Calibration with Distortion Models and Accuracy Evalution", *IEEE Trans, on Pattern Analysis and Machine Intelligence*, Vol. 14, No. 10, October 1992.
12. R. Y. Tsai, "A versatile camera calibration technique for high accuracy 3D machine vision metrology using off the shelf TV cameras and lenses", *IEEE Journal of Robotics and Automati*on, Vol. RA-3, no. 4, pp. 323-344, Aug. 1987
13. D. H. Ballard, "Computer Vision", *Prentice Hall*, 1985.